Lecture 9: Attractor and strange attractor, chaos, analysis of the Lorenz attractor, transient and intermittent chaos, the Lyapunov exponents, the Kolmogorov entropy, predictability horizon, examples of chaos, cobweb diagram and recurrence map or recurrence relation (1-D map)

Contents

Demonstration: Double pendulum, the Möbius strip.

1 The Lorenz attractor

The Lorenz system was introduced during the previous lecture. The following slides present an overview of the selected properties of the system. The bifurcation analysis is shown for varied r while keeping the other parameters constant.

SLIDES: 3–8

The Lorenz attractor

The **Lorenz attractor** has the form

$$\begin{cases} \dot{x} = d(y-x), \\ \dot{y} = rx - y - xz, \\ \dot{z} = xy - bz, \end{cases} \tag{1}$$

where r, d, and b are the parameters. For $r = 28$, $d = 10$, and $b = 8/3$, the system has a chaotic solution. Other parameter values may generate other types of solutions.

The Lorenz equations also arise in simplified models for lasers, dynamos, thermosyphons, brushless DC motors, electric circuits, chemical reactions and forward osmosis.

Properties of the Lorenz attractor

- There exists a symmetric pair of solutions. If $(x, y) \to (-x, -y)$ the system stays the same. If solution $(x(t), y(t), z(t))$ exists then solution $(-x(t), -y(t), z(t))$ is also a solution.
- The Lorenz system is **dissipative**[1]: volumes V in phase space contract under the flow. As $t \to \infty$, $V \to 0$.

$$\dot{V} = \int_V \nabla \cdot \dot{\vec{x}} \, \mathrm{d}V \tag{2}$$

$$\nabla \cdot \dot{\vec{x}} = \frac{\partial}{\partial x}[d(y-x)] + \frac{\partial}{\partial y}(rx - y - xz) + \frac{\partial}{\partial z}(xy - bz) = \\ = -(d+1+b) < 0 = \text{const.} \tag{3}$$

Since the divergence is constant, (2) reduces to

$$\dot{V} = -(d+1+b)\,V \quad \Rightarrow \quad V(t) = V(0)\mathrm{e}^{-(d+1+b)t}. \tag{4}$$

[1]See Mathematica .nb file uploaded to the course webpage.

Bifurcation analysis of the Lorenz attractor

For $r < 1$ ($d = 10$, $b = 8/3$) there is only one stable fixed point located at the origin. This point corresponds to no convection. All orbits converge to the origin — a global attractor.
A **supercritical pitchfork bifurcation** occurs at $r = 1$, and for $r > 1$ two additional fixed points appear at

$$(x^*, y^*, z^*) = C^{\pm} = \left(\pm\sqrt{\beta(r-1)}, \pm\sqrt{\beta(r-1)}, r-1\right). \tag{5}$$

These correspond to steady convection. Fixed points are stable only if

$$r < r_{\text{Hopf}}, \quad r_{\text{Hopf}} = d\,\frac{d+b+3}{d-b-1} = 24.74, \tag{6}$$

which can hold only for positive r and $d > b + 1$. At a critical value $r = r_{\text{Hopf}}$, both stable fixed points lose stability through a **subcritical Hopf** bifurcation.

Bifurcation analysis of the Lorenz attractor

As we decrease r from r_{Hopf}, the unstable limit cycles expand and pass precariously close to the **saddle point** at the origin. At $r = 13.926$ the cycles touch the saddle point and **become homoclinic orbits**; hence we have a **homoclinic bifurcation** which is referred to as the *first homoclinic explosion*. Below $r = 13.926$ there are no limit cycles.

The region $13.926 < r < 24.06$ is referred to as **transient chaos**[2] region. Here, the chaotic trajectories eventually settle at C^+ or C^-.

[2]See Mathematica .nb file uploaded to the course webpage.

Bifurcation analysis of the Lorenz attractor

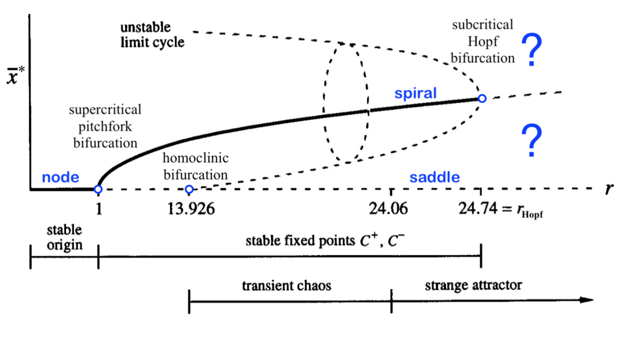

Bifurcation analysis of the Lorenz attractor

For $r > 24.06$ and $r > r_{\text{Hopf}} = 28$ (immediate vicinity): no stable limit-cycles exist; trajectories do not escape to infinity (dissipation); do not approach an invariant torus (quasi-periodicity). Almost all initial conditions (I.C.s) will tend to an invariant set — the Lorenz attractor — a **strange attractor** and a **fractal**.

Note: No quasi-periodic solutions for $r > r_{\text{Hopf}}$ are possible because of the dissipative property of the flow.

For $r \gg r_{\text{Hopf}}$ different types of chaotic dynamics exist, e.g. **noisy periodicity, transient and intermittent chaos**. One can even find transient chaos settling to periodic orbits[3].

[3]See Mathematica .nb file uploaded to the course webpage.

Slide 7 shows the behaviour for small values of r while keeping the other parameters constant. Here $\overline{x}^*$ is the distance from the origin. The origin is a globally stable node for $r < 1$. At $r = 1$ the origin loses stability by a **supercritical pitchfork bifurcation**, and a symmetric pair of attracting fixed points (stable spirals) is born, in the above schematic, only one of the pair is shown. At $r_{\text{Hopf}} = 24.74$ the fixed points lose stability by absorbing an unstable limit-cycle in a **subcritical Hopf bifurcation**. As we decrease r from r_{Hopf}, the unstable limit-cycles expand and pass precariously close to the **saddle point** at the origin. At $r = 13.926$ the cycles touch the saddle point and **become homoclinic orbits**; hence we have a **homoclinic bifurcation** of unstable limit-cycles. Below $r = 13.926$ there are no limit-cycles. Viewed in the other direction, we could say that a pair of unstable limit-cycles are created as r increases through $r = 13.926$.

NUMERICS: NB#1

Dissipative chaotic flow of the Lorenz attractor visualisation via particle tracking. Calculation of divergence of 3-D and higher dimensional flows.

Examples of the transient, intermittent and periodic dynamics in the Lorenz system for $r \gg r_{\text{Hopf}}$ ($d = 10$, $b = 8/3$) are shown in Sec. 3 where these phenomena are defined and in numerical file NB#3.

2 Exponential divergence of initially neighbouring trajectories

2.1 The Lyapunov exponents

From numerical integration of the Lorenz system we know that the flow on the attractor trajectories exhibits **sensitive dependence on initial conditions**. This means that two trajectories starting very close to each other will rapidly diverge, and thereafter have totally different futures, see Fig. 1.

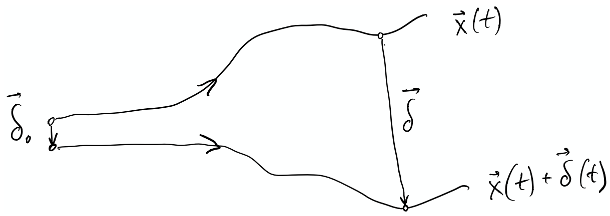

Figure 1: Rapidly diverging trajectories where the initial separation $|\vec{\delta}_0| = \delta_0 \approx 0$ and at the same time $|\vec{\delta}_0| = \delta_0 \neq 0$.

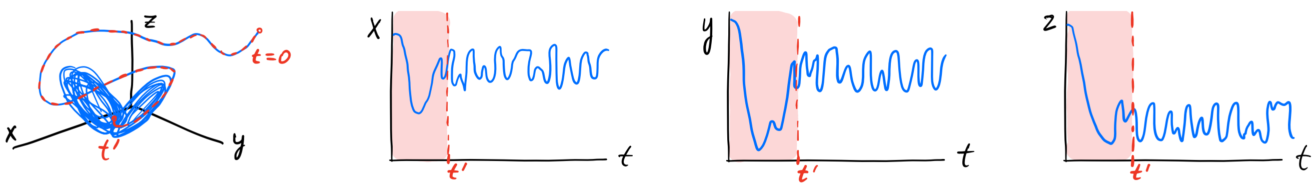

Figure 2: Sketch of a solution to the Lorenz system (Slide 3). Initial transient dynamics lasting for time period $t \in [0, t')$. Transient trajectory is shown with the dashed red and blue curve on the 3-D xyz-plot or with the pink background on the $x(t)$, $y(t)$ and $z(t)$ time-series graphs.

It can be demonstrated that after the **transient behaviour**, that is shown in Fig. 2, has elapsed, and the trajectory has settled on the **attracting set**—the Lorenz attractor, the norm (magnitude) of the separation vector $\vec{\delta}$:

$$|\vec{\delta}(t)| \sim \delta_0 \mathrm{e}^{\lambda t}, \tag{1}$$

where in the case of the Lorenz system $\lambda \approx 0.9$. Hence, neighbouring trajectories diverge exponentially fast. Equivalently, if we plot $\ln|\vec{\delta}|$ against t—a semi-logarithmic plot, we find a curve that can be approximated by a straight line with a positive slope of λ, see Fig. 3.

The exponential divergence must stop when the separation is comparable to the *diameter of the attractor* (the underlying attracting set, think the Lorenz butterfly)—the trajectories obviously can't get any farther apart than that. This explains the levelling off or **saturation** of the curve $\ln|\vec{\delta}(t)|$ shown with the horizontal grey dashed line in Fig. 3.

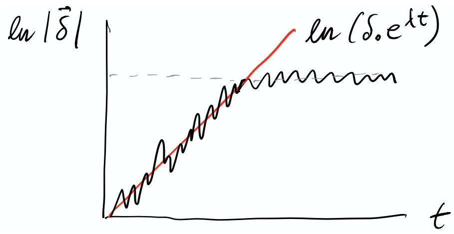

Figure 3: Norm of separation vector $|\vec{\delta}|$ as a function of t. Slope λ is shown with the straight red line.

The exponent λ is often called the **Lyapunov exponent**, although this is a sloppy use of the term, for two reasons:

- First, there are actually n different Lyapunov exponents for each degree of freedom of an n-dimensional system. We call them λ_x, λ_y, $\lambda_z, \ldots$, etc.;
- Second, λ depends slightly on which trajectory we study. We should average over many trajectories (many initial conditions) and over many different points on the same trajectory to get the true value.

The true Lyapunov exponent λ of a given system is usually close to the biggest of the exponents related to the degrees of freedom (λ_x, λ_y, $\lambda_z, \ldots$). The biggest exponent governs the resulting slope shown in Figs. 3 and 4.
Note: Positive Lyapunov exponent $\lambda > 0$ is an indicator of chaos.

NUMERICS: NB#2

The Lyapunov exponent of 3-D chaotic systems, visual demonstration.

Plotted below is the quantitatively accurate $\ln|\vec{\delta}|$ vs. t graphs shown in Fig. 3 for the Lorenz attractor with the same parameters as used in Sec. 1.

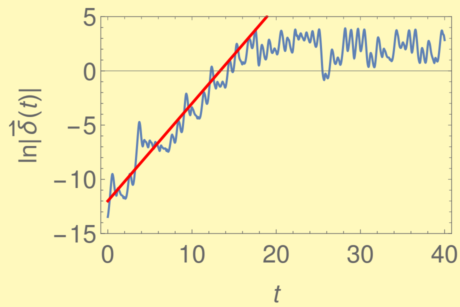

Figure 4: Exponential divergence of trajectories in the Lorenz system shown with the blue graph. The graph of $\ln(\delta_0 \mathrm{e}^{\lambda t})$ where the Lyapunov exponent $\lambda = 0.9$ is shown with the red line.

2.2 The Kolmogorov entropy

Also known as the **metric entropy**, the Kolmogorov-Sinai entropy, or KS entropy. The Kolmogorov entropy is zero for non-chaotic motion and positive for chaotic motion. For $\lambda_i > 0$ one can find the Kolmogorov entropy using the following formula:

$$K = \sum_i \lambda_i, \tag{2}$$

where i spans the number of degrees of freedom of a given system. The Kolmogorov entropy is a measure of the growth of uncertainty due to the expansion rate given by the positive Lyapunov exponents λ_i.

2.3 Predictability horizon

Predictability horizon is also called the **Lyapunov time**. When a system has a positive Lyapunov exponent λ, there is a time horizon beyond which prediction breaks down, as shown schematically in Fig. 5. After some time $t > 0$ has elapsed, the discrepancy or the difference between two solutions shown in Fig. 5, grows

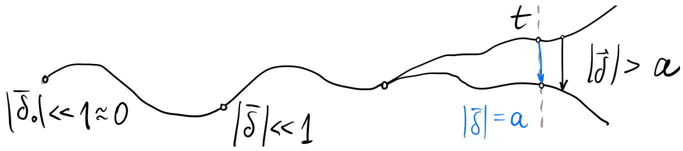

Figure 5: Deviation of two trajectories with close-by initial conditions, where a is the allowed tolerance representing a noticeable deviation from the true trajectory.

according to (1) to

$$|\vec{\delta}(t)| = \delta(t) \approx \delta_0 \mathrm{e}^{\lambda t}. \tag{3}$$

We let $|\vec{\delta}| = a$ be a measure of our tolerance, i.e., if prediction is within a of the true/nominal state, we consider it acceptable, see Fig. 5. Then our prediction becomes intolerable when $|\vec{\delta}(t)| = \delta(t) > a$. How *long* will the system be predictable, i.e., evolve within selected tolerance a? This question can be answered by solving

$$a \approx \delta_0 \mathrm{e}^{\lambda t}, \tag{4}$$

for time t:

$$\mathrm{e}^{\lambda t} \approx \frac{a}{\delta_0} \quad \Big| \ln(\,), \tag{5}$$

$$\ln \mathrm{e}^{\lambda t} \approx \ln \frac{a}{\delta_0}, \tag{6}$$

$$\lambda t \approx \ln \frac{a}{\delta_0}, \quad \Big| \div \lambda, \tag{7}$$

$$\boxed{t \approx \frac{1}{\lambda} \ln \frac{a}{\delta_0}.} \tag{8}$$

As stated above we refer to this time interval as the **predictability horizon** or simply the **Lyapunov time**. The **characteristic time scale** (or order) of chaos thus is:

$$O(t) \approx O\left(\frac{1}{\lambda} \ln \frac{a}{\delta_0}\right) \approx O\left(\frac{1}{\lambda} \cdot 1\right) \approx O\left(\frac{1}{\lambda}\right). \tag{9}$$

At time scales $1/\lambda$ chaos becomes noticeable. The trajectories deviate beyond acceptable tolerance.

Slides: 9, 10

The Lyapunov exponent and predictability horizon

Example: Suppose we're trying to predict the future state of a chaotic system within a tolerance of $a = 10^{-3}$. Given that our estimate of the initial state is uncertain to within $\delta_0 = 10^{-7}$, for about how long can we predict the state of the system, while remaining within the tolerance?

Now suppose we manage to measure the initial state a *million* times better, i.e., we improve our initial error to $\delta_0 = 10^{-13}$. How much longer can we predict?

D. Kartofelev YFX1560 9 / 40

The Lyapunov exponent and predictability horizon

Solution: The original prediction has

$$t = \frac{1}{\lambda} \ln \frac{10^{-3}}{10^{-7}} = \frac{1}{\lambda} \ln(10^4) = \frac{4 \ln 10}{\lambda}. \tag{7}$$

The improved prediction has

$$t = \frac{1}{\lambda} \ln \frac{10^{-3}}{10^{-13}} = \frac{1}{\lambda} \ln(10^{10}) = \frac{10 \ln 10}{\lambda}. \tag{8}$$

Thus, after a millionfold improvement in our initial uncertainty, we can predict only $10/4 = 2.5$ times longer (system's timeframe)!

Conclusions: If one wants to predict further into the future the task becomes exponentially *harder*. Since,

$$t \simeq \frac{1}{\lambda} \ln \frac{a}{\delta_0} \sim \ln \frac{a}{\delta_0} \quad \Rightarrow \quad \frac{a}{\delta_0} \sim \mathrm{e}^t. \tag{9}$$

D. Kartofelev YFX1560 10 / 40

The logarithmic dependence on δ_0 is what hurts us. No matter how hard we work to reduce the initial measurement error, we can't predict longer than a **few multiples of** $1/\lambda$. If you want to predict further into the future by increasing the Lyapunov time for given a the task becomes exponentially harder requiring ever-smaller δ_0 values because $a/\delta_0 \sim \mathrm{e}^t$, see Slide 10, Eq. (9). Figure 6 shows this exponential dependance.

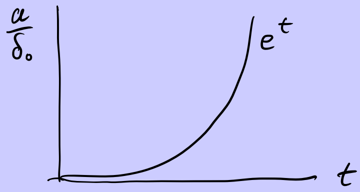

Figure 6: Ratio a/δ_0 dependence on the Lyapunov time t.

Note: The above conclusions hold for all integration methods. In fact, a *bad* numerical method may worsen the situation significantly. Even if you have an analytic solution, it too will have the predictability horizon, because you are still required to input an initial condition—a number with finite accuracy (significant figures in a decimal fraction) to generate a solution.

Question: Let's assume we are somehow able to eliminate the measurement error or/and are able to input initial conditions with absolute accuracy, i.e., $\delta_0 = 0$. Will this make a chaotic system predictable in practice?

The Lyapunov time given by (8) for the aforementioned assumption is the following:

$$t = \lim_{\delta_0 \to 0} t = \lim_{\delta_0 \to 0} \left(\frac{1}{\lambda} \ln \frac{a}{\delta_0} \right) = \infty. \tag{10}$$

This result suggest that the chaotic problem becomes predictable. The answer to the above question is "yes." Unfortunately, the above assumptions are utterly unrealistic.

NUMERICS: NB#3

Demonstration of the effect of calculation accuracy and precision on the numerical solution and the predictability horizon of a chaotic system. Transient and intermittent chaos.

By now it should be obvious that chaotic solutions are also **sensitive to numerical precision and accuracy of numerical integration**. The numerical accuracy is related to the number of significant figures or even to a specific floating point representation of real numbers themselves used in calculations by a computer. **Obtaining long-term true trajectories of chaotic dynamical systems by means of numerical methods is generally speaking not a trivial task.**

3 Conceptual definition of chaos and strange attractor

SLIDE: 11

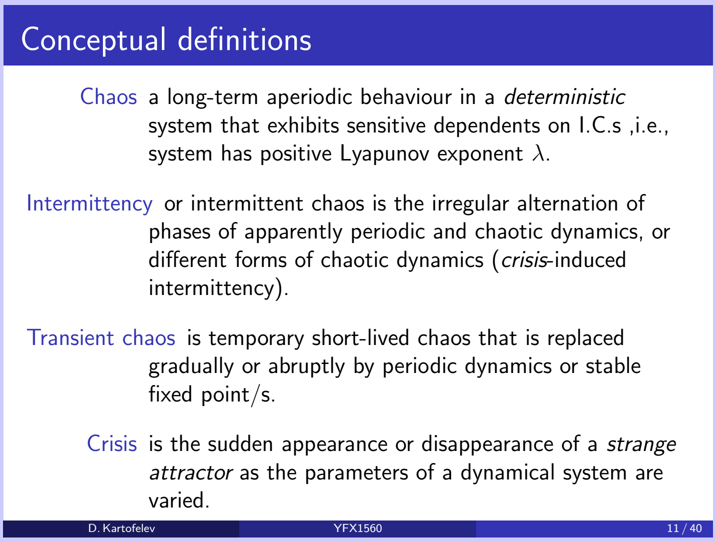

Simple examples of **transient chaos** are the dynamics of dice throws and casino roulette.

As mentioned in Sec. 1 and Slide 8, transient chaos and intermittent chaos regimes are present in the Lorenz system. The following numerical file demonstrates them in action.

NUMERICS: NB#3

Demonstration of the effect of calculation accuracy and precision on the numerical solution and the predictability horizon of a chaotic system. Transient and intermittent chaos.

Showing the transient chaos, intermittent chaos and long-term periodic limit-cycle present in the Lorenz system *cf.* Slide 7.

SLIDES: 12, 13

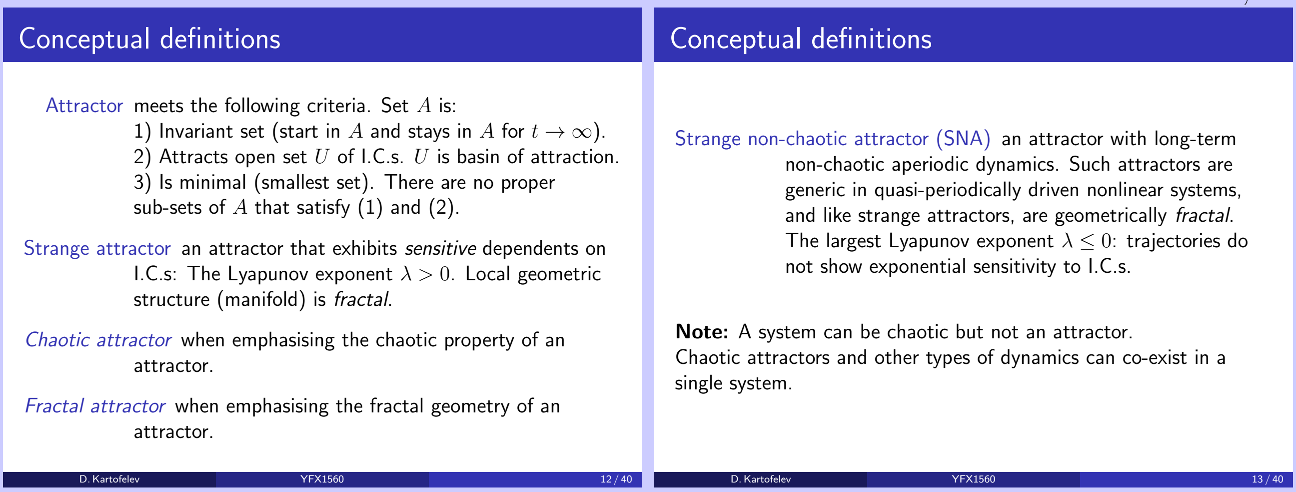

A dynamic system with a chaotic attractor is **locally unstable yet globally stable**: once some trajectories have entered the attractor, nearby points diverge from one another but never depart from the attractor. The dynamics inside the chaotic attractors is peculiar it manages to **combine attracting flow with exponential divergence of the same flow**. In future lectures this seemingly paradoxical situation will be further explored. The term strange attractor was coined by David Ruelle and Floris Takens to describe the attractor resulting from a series of bifurcations of a system describing fluid flow.

The Lorenz system is a strange attractor. The formal proof of the Lorenz system being a strange attractor is outside the scope of our course.

3.1 Identifying attractors

Determine if the following dynamics feature (non-chaotic) attractors.

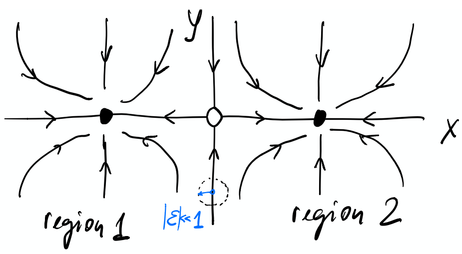

Figure 7: Two-dimensional phase portrait featuring two stable nodes and a saddle located at the origin. y-axis as a set contains its boundary thus is not an open set.

3.1.1 Example 1

Figure 7 shows the first example. Let's evaluate all possible candidates:

- origin: violates criterion 2
- y-axis: violates criterion 2
- x-axis: violates criteria 2, 3
- stable nodes: satisfy all criteria in regions 1 and 2 that are shown in Fig. 7

Conclusion: The stable nodes are attractors and regions 1 and 2 are their respective attracting sets.

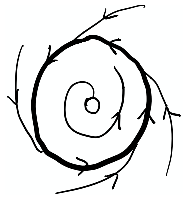

Figure 8: Stable limit-cycle on the plane where the unstable spiral is at the origin.

Figure 9: (Left) Half-stable limit-cycle on the plane where the unstable spiral is at the origin. (Right) Half-stable limit-cycle defines a closed set because it contains its boundary.

3.1.2 Example 2

Figure 8 shows the second example. Let's evaluate all possible candidates:

- origin: violates criterion 1
- limit-cycle (basin of attraction $\mathbb{R}^2 - (0,0) \in \mathbb{R}^0$ is an open set): satisfies all criteria

Conclusion: The stable limit-cycle is an attractor and $\mathbb{R}^2 - (0,0) \in \mathbb{R}^0$ is the attracting set.

3.1.3 Example 3

Figure 9 shows the third example. Let's evaluate all possible candidates:

- origin: violates criterion 1
- limit-cycle (attracting region inside of the limit-cycle $-(0,0) \in \mathbb{R}^0$): violates criterion 2

Conclusion: The half-stable limit-cycle is not an attractor (no open attracting sets found).

3.2 Selected examples of strange attractors

The strange attractors shown on the following slides and integrated in the numerical file linked below have been either designed as purely abstract mathematical objects or they have arisen across different scientific disciplines.

Slides: 14–20

The Rössler attractor

The **Rössler attractor**[4] has the form

$$\begin{cases} \dot{x} = -y - x, \\ \dot{y} = x + ay, \\ \dot{z} = b + z(x - c). \end{cases} \tag{10}$$

Chaotic solution exists for $a = 0.1$, $b = 0.1$, $c = 14$.

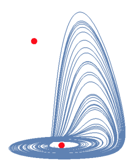

[4]See Mathematica .nb file uploaded to the course webpage.

D. Kartofelev YFX1560 14 / 40

The Chen attractor

The **Chen attractor**[5] has the form

$$\begin{cases} \dot{x} = a(y - x), \\ \dot{y} = (c - a)x - xz + cy, \\ \dot{z} = xy - bz. \end{cases} \tag{11}$$

Chaotic solution exists for $a = 35$, $b = 3$, $c = 28$.

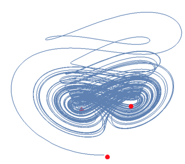

[5]See Mathematica .nb file uploaded to the course webpage.

D. Kartofelev YFX1560 15 / 40

The Rössler attractor has only one nonlinearity, namely the term zx, in the third equation. For a long time it was thought to be the algebraically simplest chaotic attractor.

The modified Chen attractor

The **modified Chen attractor**[6] has the form

$$\begin{cases} \dot{x} = a(y - x), \\ \dot{y} = (c - a)x - xz + cy + m, \\ \dot{z} = xy - bz. \end{cases} \tag{12}$$

Chaotic solution exists for $a = 35$, $b = 3$, $c = 28$, $m = 23.1$.

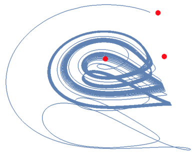

[6] See Mathematica .nb file uploaded to the course webpage.

D. Kartofelev YFX1560 16 / 40

The Lü attractor

The **Lü attractor**[7] has the form

$$\begin{cases} \dot{x} = a(y - x), \\ \dot{y} = -xz + cy, \\ \dot{z} = xy - bz. \end{cases} \tag{13}$$

Chaotic solution exists for $a = 36$, $b = 3$, $12.7 < c < 17.0$ (similar to the Lorenz system), $23.0 < c < 28.5$ (similar to the Chen system).

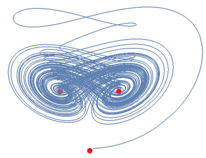

[7] See Mathematica .nb file uploaded to the course webpage.

D. Kartofelev YFX1560 17 / 40

The Pan-Xu-Zhou attractor

The **Pan-Xu-Zhou attractor**[8] has the form

$$\begin{cases} \dot{x} = a(y - x), \\ \dot{y} = cx - xz, \\ \dot{z} = xy - bz. \end{cases} \tag{14}$$

Chaotic solution exists for $a = 10$, $b = 8/3$, $c = 16$.

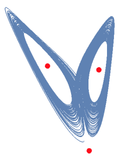

[8] See Mathematica .nb file uploaded to the course webpage.

D. Kartofelev YFX1560 18 / 40

The Bouali attractor

The **Bouali attractor**[9] has the form

$$\begin{cases} \dot{x} = \alpha(1 - x)x - \beta z, \\ \dot{y} = -\gamma(1 - x^2)y, \\ \dot{z} = \mu x. \end{cases} \tag{15}$$

Chaotic solution exists for example for $\alpha = 3.0$, $\beta = 2.2$, $\gamma = 1.0$ and $\mu = 0.001$.

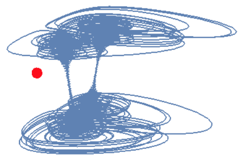

[9] See Mathematica .nb file uploaded to the course webpage.

D. Kartofelev YFX1560 19 / 40

Strange attractors

Some other strange attractors:

- The Lorenz 84 attractor
- The Newton–Leipnik chaotic system
- The Thomas' cyclically symmetric attractor
- The Sprott attractors (Sprott A – S)
- The algebraically simplest dissipative chaotic flow (based on jerk equation derived by J. S. Sprott)

$$\dddot{x} + A\ddot{x} \pm \dot{x}^2 + x = 0, \tag{16}$$

where A is constant taken as 2.017, for example.

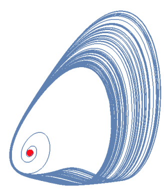

Figure: The algebraically simplest dissipative chaotic flow.

D. Kartofelev YFX1560 20 / 40

Topology of the attracting set of the algebraically simplest chaotic flow (16) is the **Möbius strip**.
Demonstration: The Möbius strip.

Numerics: NB#4

Numerical solutions of chaotic systems: the Lorenz attractor, the Rössler attractor, the Chen attractor, the modified Chen attractor, the Lu attractor, the Pan-Xu-Zhou attractor, the Bouali attractor, and the algebraically simplest chaotic dissipative flow by J. C. Sprott.

3.3 Examples of chaotic systems

Systems can be chaotic without explicitly containing one or being a strange attractor similar to the ones shown above. In this section we introduce three chaotic phenomena, the systems describing them and their numerical solutions. The selected examples are the following:

- Double pendulum.
- Magnetic pendulum in three magnetic potentials.
- The planar three-body problem.

Figure 10: Double pendulum used in the classroom during the demonstration.

Demonstration: Ask students to repeat the dynamics of the double pendulum motion via repeated selection of pendulum's initial position. Figure 10 shows the double pendulum used during the classroom demonstration.

SLIDES: 21, 22

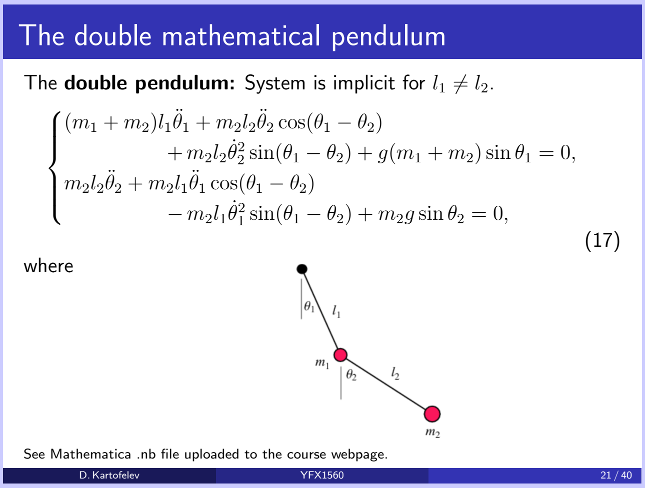

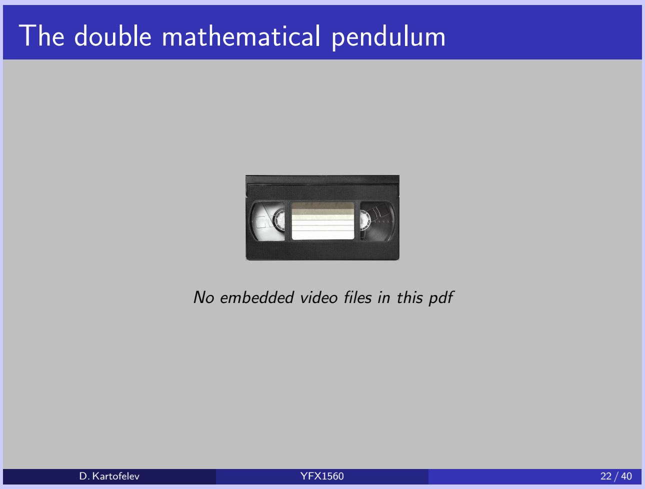

NUMERICS: NB#5

Numerical solutions of chaotic systems: double mathematical pendulum with one and two sets of initial conditions. Phase portrait of the double pendulum system.

SLIDES: 23–30

Magnetic pendulum in three magnetic potentials

System is modeled with the following equations of motion:

$$\begin{cases} \ddot{x} + R\dot{x} - \displaystyle\sum_{i=1}^{N} \frac{x_i - x}{\left(\sqrt{(x_i - x)^2 + (y_i - y)^2 + d^2}\right)^3} + Cx = 0, \\ \ddot{y} + R\dot{y} - \displaystyle\sum_{i=1}^{N} \frac{y_i - y}{\left(\sqrt{(x_i - x)^2 + (y_i - y)^2 + d^2}\right)^3} + Cy = 0, \end{cases} \tag{18}$$

where R is proportional to the air resistance and overall attenuation, C is proportional to the effects of gravity, N is the number of magnets, the i-th magnet is positioned at (x_i, y_i), d is the distance between the pendulum at rest and the plane of magnets.

Additionally we assume that the pendulum length is long compared to the spacing of the magnets. Thus, we may assume for simplicity that the metal ball moves about on a xy-plane.

D. Kartofelev YFX1560 23 / 40

Magnetic pendulum in three magnetic potentials[10]

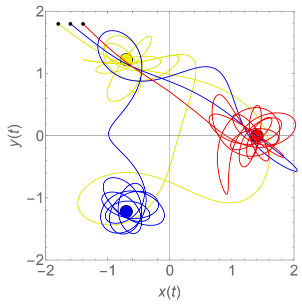

Figure: Magnets shown with the yellow, red and blue colours, attracting the magnetic pendulum for three neighbouring initial conditions.

[10] See Mathematica .nb file uploaded to the course webpage (Lecture №1).

D. Kartofelev YFX1560 24 / 40

In addition to sensitivity to initial conditions this system features the so-called **final-state sensitivity**. This phenomenon may occur whenever there are **several coexisting attractors**. These may be strange attractors or perhaps simply attractive fixed points (as is the case here). The trajectory for a given initial position will typically converge to one of the attractors. Therefore, there must be a boundary of the corresponding basins of attractions. Such boundaries often are *fractals* as can be seen below.

How to classify this system? The three magnets taken as separate attractors or all magnets taken as a single attractor (an attracting set containing three fixed points) satisfy the definition of an attractor. Local geometry of these attractors is not *fractal* making them not strange. Additionally, the dynamics is also not long-term sustainable because all trajectories eventually stop at one of the magnets due to the attenuation terms present in the system. We conclude that the dynamics is the **final-state sensitive transient chaos**.

Magnetic pendulum

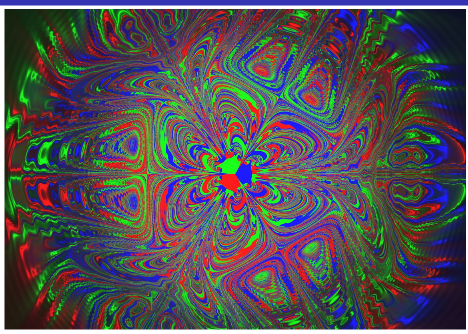

Figure: The **basins of attraction** of the three magnets which are coloured red, blue and green.

D. Berger, `https://twitter.com/InertialObservr`

D. Kartofelev YFX1560 25 / 40

Magnetic pendulum

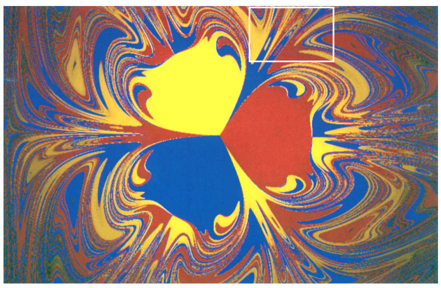

Figure: The **basins of attraction** of the three magnets which are coloured red, blue and yellow.

H. Peitgen, *et al*, *Chaos and Fractals: New Frontiers of Science*, Springer-Verlag, 2004, pp. 707–714.

D. Kartofelev YFX1560 26 / 40

Magnetic pendulum

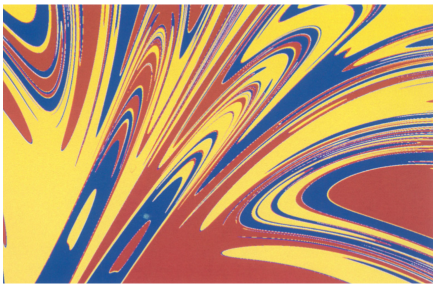

Figure: Detail of previous slide showing the intertwined structure of the three basins.

H. Peitgen, *et al*, *Chaos and Fractals: New Frontiers of Science*, Springer-Verlag, 2004, pp. 707–714.

D. Kartofelev YFX1560 27 / 40

The gravitational three-body problem

The **gravitational three-body problem**[11]: system consists of 18 first order equations.

$$\ddot{\vec{r}}_i = \sum_{j=1, j\neq i}^{3} -Gm_j \frac{\vec{r}_i - \vec{r}_j}{|\vec{r}_i - \vec{r}_j|^3}, \quad i = 1, 2, 3, \tag{19}$$

where $\vec{r}_i = (x_i, y_i, z_i)$ is the ith body's position vector, $\ddot{\vec{r}}_i$ is the acceleration of ith body, m_j is the jth mass, $\vec{r}_i - \vec{r}_j$ is the vector connecting the masses i and j, G is the gravitational constant, and $|\vec{\alpha}|$ denotes the vector norm of vector $\vec{\alpha}$.

[11] See Mathematica .nb file uploaded to the course webpage. Numerical solution of the planar problem where $\vec{r}_i = (x_i, y_i)$ is uploaded.

D. Kartofelev YFX1560 28 / 40

The gravitational three-body problem[12]

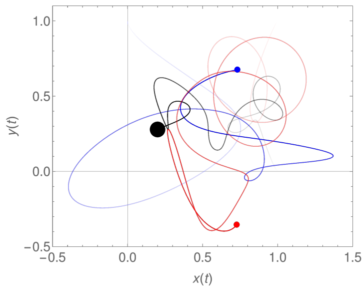

Figure: Numerical solution of the planar three-body problem.

[12] See Mathematica .nb file uploaded to the course webpage. Numerical solution of the planar problem where $\vec{r}_i = (x_i, y_i)$ is uploaded.

D. Kartofelev YFX1560 29 / 40

Dynamics of the Solar System

Is our solar system chaotic or not?

Read: J. Laskar, "Large-scale chaos in the solar system," *Astronomy and Astrophysics*, **287**(1), pp. L9–L12, (1994).

Consider also other works by J. Laskar.

Read: Wayne B. Hayes, Anton V. Malykh, Christopher M. Danforth, "The interplay of chaos between the terrestrial and giant planets," *Monthly Notices of the Royal Astronomical Society*, **407**(3), pp. 1859–1865, (2010).

D. Kartofelev YFX1560 30 / 40

In our planetary system the planets' orbits are chaotic over long timescales, whole Solar System possesses the **Lyapunov time in the range of 2–230 million years**. This means that the position of a planet along its orbit ultimately becomes impossible to predict with any certainty, e.g., the timing of winter and summer on any given planet becomes uncertain. In some cases the orbits themselves may change *dramatically*. Such chaos manifests most strongly as changes in eccentricity, with some planets' orbits becoming significantly more elliptical or less elliptical. The topic of Solar System's stability on time scales of many billions of years is outside the scope of this course.

NUMERICS: NB#6

Numerical solutions of chaotic systems: the gravitational three body problem (planar). Interactive code with several dynamic visualisation styles.

Reading suggestion

Link	File name	Citation
Paper#1	paper1b.pdf	Jacques Laskar, "Large-scale chaos in the solar system," *Astronomy and Astrophysics*, **287**(1), pp. L9–L12, (1994). Stable URL: http://adsabs.harvard.edu
Paper#2	paper1c.pdf	Wayne B. Hayes, Anton V. Malykh, Christopher M. Danforth, "The interplay of chaos between the terrestrial and giant planets," *Monthly Notices of the Royal Astronomical Society*, **407**(3), pp. 1859–1865, (2010). doi:10.1111/j.1365-2966.2010.17027.x

4 A brief introduction to 1-D maps

Maps are also called **recursion relations**, **recursion maps**, or **iterated maps**.

SLIDES: 31, 32

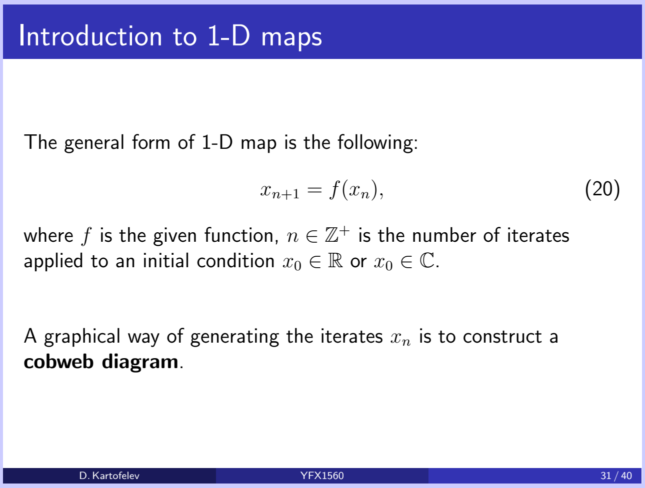

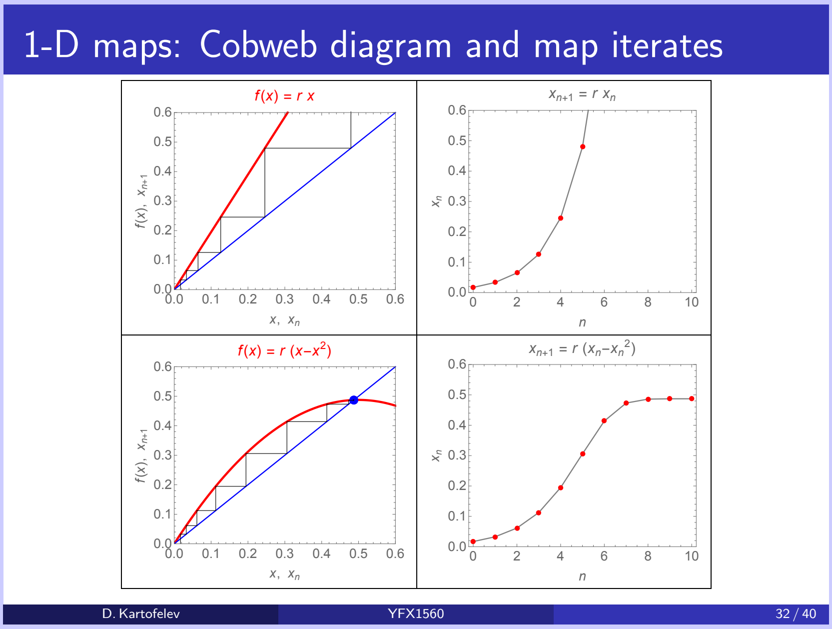

To construct a **cobweb diagram** one ideally selects an <u>initial condition x_0 in the basin of the map</u>. The **basin** of a map includes values x_n that return other points on the same map and not the infinity. Map iterates can be found graphically: **move vertically to the function $f(x)$ and register the result, move horizontally to the diagonal** and repeat. The resulting map iterates x_n are shown on Slide 32.

The map shown in the upper row of the graphs shown on Slide 32, has the following form:

$$x_{n+1} = rx_n, \tag{11}$$

here $r > 1$ is the control parameter. This map has no map basin. The iterates $x_n \to \infty$ for $n \to \infty$. The graphs in the lower row are based on a map given in the form:

$$x_{n+1} = r\left(x_n - x_n^2\right), \tag{12}$$

where $r > 0$ is the control parameter. This map has a map basin since the map iterates x_n remain bounded for $n \to \infty$ and don't escape to infinity. A more detailed analysis of map iterate dynamics will be presented in future lectures.

The code used to generate the cobweb diagrams shown on Slide 32 is linked below.

Numerics: NB#7

Introduction to cobweb diagramming. Interactive cobweb diagrams of 1-D maps $x_{n+1} = rx_n$ and $x_{n+1} = r\left(x_n - x_n^2\right)$ where r is the control parameter.

5 Dynamics of the Lorenz attractor in the chaotic regime

Our goal in this section is to demonstrate that the Lorenz attractor is indeed *chaotic*. Surprisingly, we can use a one-dimensional mapping of the chaotic flow of the Lorenz system to do so.

Slides: 33–35

Chaotic dynamics in the Lorenz attractor

How do we know that the Lorenz attractor is not just a stable limit-cycle in disguise?

Playing devil's advocate, a skeptic might say, "Sure, the trajectories don't ever seem to repeat, but maybe you haven't integrated long enough. Eventually the trajectories will settle down into a periodic behaviour — it just happens that the **period is incredibly long**, much longer than you've tried in your computer. Prove me wrong."

D. Kartofelev YFX1560 33 / 40

Chaotic dynamics in the Lorenz attractor

Lorenz directs our attention to a particular view of the attractor.

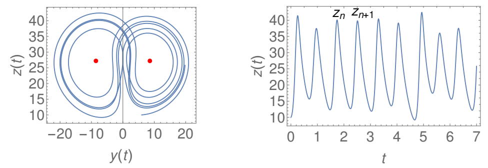

Lorenz writes: "the trajectory apparently leaves one spiral only after exceeding some critical distance from the center. Moreover, the extent to which this distance is exceeded appears to determine the point at which the next spiral is entered; this in turn seems to determine the number of circuits to be executed before changing spirals again. It therefore seems that some single feature of a given circuit should predict the same feature of the following circuit." (Lorenz 1963)

The feature that he focuses on is z_n the n-th local maximum of $z(t)$.

D. Kartofelev YFX1560 34 / 40

Chaotic dynamics in the Lorenz attractor

Lorenz's idea is that z_n should predict z_{n+1}. To check this, he numerically integrated the equations for $t \gg 1$, then found the local maxima of $z(t)$, and finally plotted z_{n+1} vs. z_n. The data from the chaotic time series appear to fall neatly on a curve.

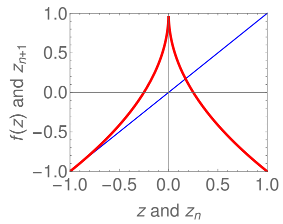

Figure: The Lorenz map shown with red where $|f'(z)| > 1$ for $\forall z \neq 0$.

By this ingenious trick, Lorenz was able to extract order from chaos. The normalised map $z_{n+1} = f(z_n)$ shown above is now called the **Lorenz map**.

D. Kartofelev YFX1560 35 / 40

When we say $|f'(z)| > 1$ for $\forall z \neq 0$ we mean only the values that are in the **basin of the map**, i.e., the values that return other points on the map and don't escape to infinity, see Sec. 4.

The following numerical file contain an interactive cobweb diagram of the Lorenz map iterates.

Numerics: NB#8

Interactive cobweb diagram and iterates of the Lorenz map.

How neatly does the actual local maxima of $z(t)$ fall on the curve $f(z)$ shown on Slide 35? It depends on the selection of system parameters and initial conditions. In the numerical file linked below one such example is shown.

NUMERICS: NB#9

The Lorenz map: quantitatively accurate Lorenz mapping.

Figure 11 shows the long-term dynamics where $t \leq 150$ of the local maxima z_n of $z(t)$ for parameter values $\sigma = 10$, $\rho = 28$, $\beta = 8/3$, and initial condition $x_0 = x(0) = 19$, $y_0 = y(0) = 20$, $z_0 = z(0) = 50$.

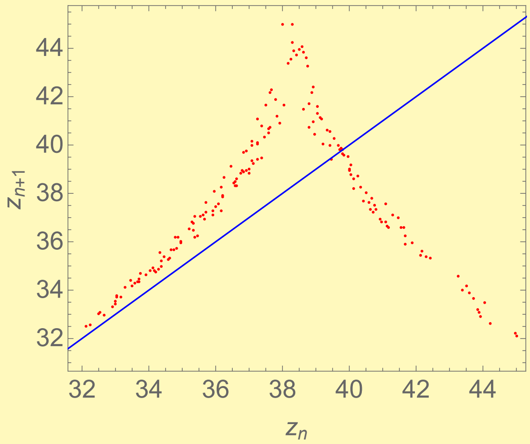

Figure 11: The Lorenz mapping for selected parameter and initial condition values. The blue diagonal corresponds to $z_{n+1} = z_n$.

The graph shown on Slide 35 is not actually a curve. It does have some *thickness* as can be seen in Fig. 11. So strictly speaking, $f(z)$ is not a well-defined function, because there can be more than one output z_{n+1} for a given input z_n. On the other hand, the thickness is *small*, and there is so much to be gained by treating the graph as a curve, that we will simply make this approximation, keeping in mind that the subsequent analysis is plausible but not rigorous.

Note: The Lorenz map or mapping is not the same as the Poincare mapping (topic discussed in Lecture 11). In both cases we're trying to simplify the analysis of a differential equation by reducing it to an iterated map of some kind. But there's an important distinction: To construct a Poincare map for a three-dimensional flow, we compute a trajectory's successive intersections with a two-dimensional surface. The Poincare map takes a point on that surface, specified by two coordinates, and then tells us how those two coordinates change after the first return to the surface. The Lorenz map is different because it characterises the trajectory by only one number, not two. This simpler approach works only if the attractor is very "flat," i.e., close to two-dimensional, as the Lorenz attractor is.

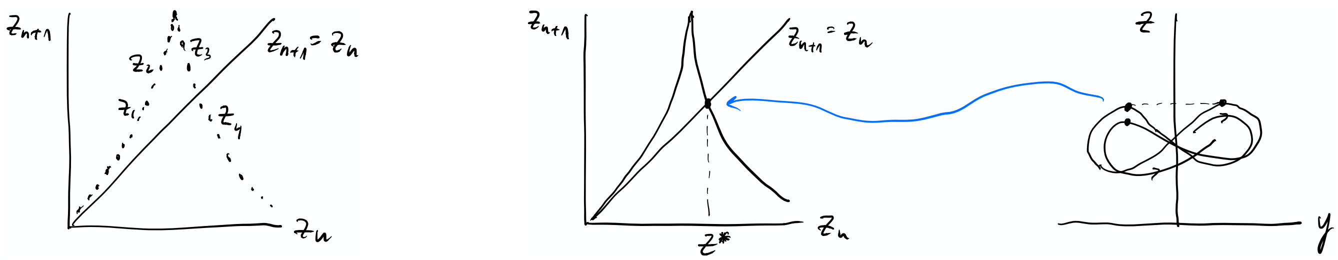

Figure 12: (Left) Local maxima z_n of time series $z(t)$ as they appear in an irregular order on the Lorenz map. (Middle) Fixed point z^* returns the same point after an iteration. (Right) Meaning of the fixed point z^* as show on the yz-projection of the Lorenz attractor.

Figure 12 shows how the local maxima of $z(t)$ populate the Lorenz map and how fixed point z^* returns the same value after an iteration that corresponds to the spiral/orbit of a trajectory in the xyz-space (not a correct assumption). Arguably, $z_n = z^*$ does so because it lies on the diagonal where $z_{n+1} = z_n$. Theoretically, this should imply that

$$f(z^*) = z^*, \tag{13}$$

where function or map f is the analytic form of the Lorenz map. If fixed point z^* is shown to be unstable, then it must follow that the <u>underlying dynamics of the Lorenz system is aperiodic</u>. We analyse the fixed point z^* using linearisation.

SLIDES: 36, 37

Ruling out stable limit-cycles

Stability of fixed point z^* can be determined by linearisation, consider a slightly perturbed trajectory close to fixed point z^*

$$z_n = z^* + \eta_n, \tag{21}$$

where $|\eta| \ll 1$. Linearisation of the map at z^* yields

$$z_{n+1} = f(z_n) = f(z^* + \eta_n) = \begin{bmatrix}\text{Taylor series expansion}\\ \text{about } z_n = z^*\end{bmatrix} =$$
$$= f(z^*) + \frac{f'(z^*)}{1!}(z^* + \eta_n - z^*) + O(\eta_n^2) \approx z^* + f'(z^*)\eta_n. \tag{22}$$
$$\underbrace{z_{n+1} - z^*}_{\eta_{n+1}} \approx f'(z^*)\eta_n \tag{23}$$

D. Kartofelev YFX1560 36 / 40

Figure 13 shows the slightly perturbed trajectory (21) in relation to fixed point z^* and its iterates.

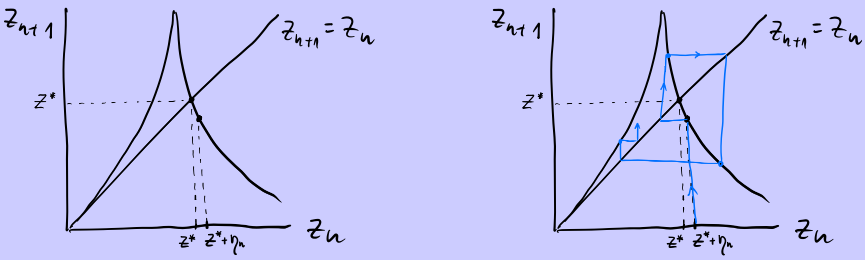

Figure 13: (Left) The Lorenz map featuring a slightly perturbed iterate $z_n = z^* + \eta_n$ where $|\eta_n| \ll 1$. (Right) Slightly perturbed iterate z_0 and a couple of consequent iterates—a cob web diagram.

Ruling out stable limit-cycles

Linearisation of the map at z^* yields

$$\boxed{\eta_{n+1} \approx |f'(z^*)|\eta_n} \tag{24}$$

Since $|f'(z^*)| > 1$, by the Lorenz map property, we get

$$|\eta_{n+1}| > |\eta_n|. \tag{25}$$

Hence, the deviation η_n grows with each iteration. Fixed point z^* is unstable, and all orbits must be unstable.
General conclusions from linearisation:

$$|f'(z^*)| < 1, \quad z^* \text{ is stable.} \tag{26}$$
$$|f'(z^*)| = 1, \quad z^* \text{ participates in bifurcation.} \tag{27}$$
$$|f'(z^*)| > 1, \quad z^* \text{ is unstable.} \tag{28}$$

D. Kartofelev YFX1560 37 / 40

The instability of fixed point z^* can be checked against the numerically obtained cobweb diagram linked below.

NUMERICS: NB#8

Interactive cobweb diagram and iterates of the Lorenz map.

The linear analysis is true. The initial condition $z_0 \approx z^*$ does not evolve towards the fixed point z^* for iterates $n > 0$. All close-by trajectories are repelled. The cobweb diagram exhibits **sensitive dependence on initial conditions**. The Lorenz map has retained the underlying chaotic properties of the Lorenz system.

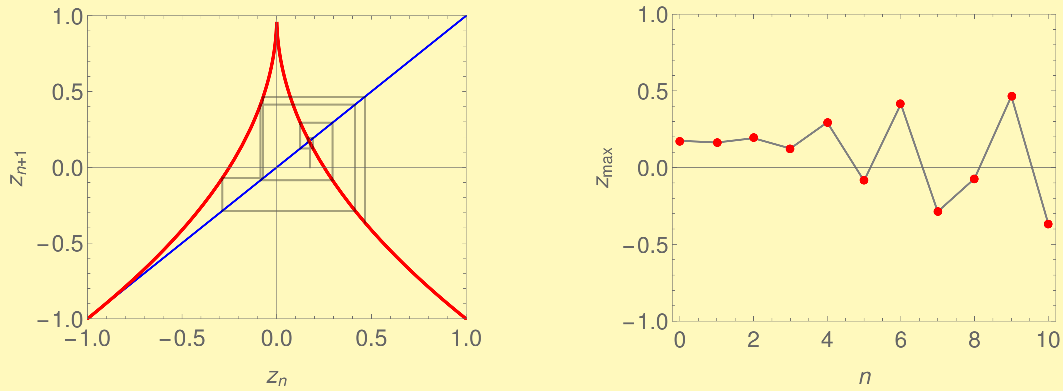

Figure 14: (Left) Cobweb diagram of the normalised Lorenz map showing the first ten iterates for $z_0 \approx z^*$. (Right) The Lorenz map iterates corresponding to the cobweb diagram shown on the left.

We finish this lecture with two open-ended questions that will be answered in the next week's lecture: Can trajectories in the Lorenz map's cobweb diagram close onto themselves? How does a closed trajectory in the cobweb diagram translate into the three-dimensional Lorenz flow?

Revision questions

1. Define attractor.
2. Define strange attractor.
3. What is the difference between a strange attractor and an attractor?
4. Name properties of the Lorenz attractor.
5. What are the Lyapunov exponents?
6. What is the Lyapunov exponent?
7. What determines the number of Lyapunov exponents?
8. What is the Kolmogorov entropy?
9. What is predictability horizon?
10. What is the Lyapunov time?
11. Can a long-term solution to a chaotic system be predicted? Explain.
12. List some examples of chaos in nature.
13. What is final-state sensitivity?
14. What is chaos?
15. What is intermittent chaos?
16. What is transient chaos?
17. What is crisis?
18. What is strange non-chaotic attractor?